PHYSICAL REVIEW LETTERS **128,** 216801 (2022)

# Zero Magnetic Field Plateau Phase Transition in Higher Chern Number Quantum Anomalous Hall Insulators

Yi-Fan Zhao,[†] Ruoxi Zhang,[†] Ling-Jie Zhou, Ruobing Mei, Zi-Jie Yan,
Moses H. W. Chan, Chao-Xing Liu, and Cui-Zu Chang[*]
*Department of Physics, The Pennsylvania State University, University Park, Pennsylvania 16802, USA*

(Received 29 September 2021; accepted 6 May 2022; published 27 May 2022)

The plateau-to-plateau transition in quantum Hall effect under high magnetic fields is a celebrated quantum phase transition between two topological states. It can be achieved by either sweeping the magnetic field or tuning the carrier density. The recent realization of the quantum anomalous Hall (QAH) insulators with tunable Chern numbers introduces the channel degree of freedom to the dissipation-free chiral edge transport and makes the study of the quantum phase transition between two topological states under zero magnetic field possible. Here, we synthesized the magnetic topological insulator (TI)/TI pentalayer heterostructures with different Cr doping concentrations in the middle magnetic TI layers using molecular beam epitaxy. By performing transport measurements, we found a potential plateau phase transition between $C = 1$ and $C = 2$ QAH states under zero magnetic field. In tuning the transition, the Hall resistance monotonically decreases from $h/e^2$ to $h/2e^2$, concurrently, the longitudinal resistance exhibits a maximum at the critical point. Our results show that the ratio between the Hall resistance and the longitudinal resistance is greater than 1 at the critical point, which indicates that the original chiral edge channel from the $C = 1$ QAH state coexists with the dissipative bulk conduction channels. Subsequently, these bulk conduction channels appear to self-organize and form the second chiral edge channel in completing the plateau phase transition. Our study will motivate further investigations of this novel Chern number change-induced quantum phase transition and advance the development of the QAH chiral edge current-based electronic and spintronic devices.

DOI: 10.1103/PhysRevLett.128.216801

A rich topic of research in condensed matter physics is to create, manipulate, and understand the quantum phase transition between two different topological states [1,2]. The quantum anomalous Hall (QAH) effect is a prime example of topological states and can be considered as a zero magnetic field manifestation of the quantum Hall effect. The QAH effect, usually realized by time-reversal symmetry breaking in topological nontrivial systems [3–7], possesses a quantized Hall resistance of $h/Ce^2$ with spin-polarized dissipation-free chiral edge channels, where $C$, known as the Chern number, corresponds to the number of chiral edge channels [8–10]. Therefore, the QAH effect may have considerable impact on future electronic and spintronic device applications for ultralow-power consumption. In 2013, the QAH effect was realized in Cr-doped topological insulator (TI) $(\mathrm{Bi,Sb})_2\mathrm{Te}_3$ films [5]. Two years later in the V-doped TI system, contrary to the prediction from the first-principle calculations [4], a high-precision QAH effect was also demonstrated [11,12]. To date, other than a few exceptions [10,13], most experiments concentrate on $C = 1$ QAH systems [5,9,11,12,14–29].

Recently, the QAH insulators with tunable $C$ have been demonstrated in magnetic TI/TI multilayers [10]. A specific magnetic TI/TI pentalayer (i.e., a magnetic TI/TI/magnetic TI/TI/magnetic TI multilayer) shows either the $C = 1$ QAH effect for the lower magnetic doping concentration or the $C = 2$ QAH effect for the higher magnetic doping concentration. This Chern number change in QAH insulators is determined by the strength of the coupling between two adjacent $C = 1$ QAH layers, which is primarily induced by the transformation of the middle magnetic TI layer from being topological nontrivial to trivial [10]. Since the magnetic doping concentration can be varied systematically, it is feasible to create a $C$ change-induced quantum phase transition between $C = 1$ and $C = 2$ QAH states by precisely altering the dopant concentration in the middle magnetic TI layer. The creation of such a $C$ change-induced quantum phase transition under zero magnetic field facilitates the development of chiral edge current-based high-capacity circuits interconnects in energy-efficient electronic and spintronic devices. Moreover, a more thorough understanding of such a zero magnetic field plateau phase transition enables the inquiry of the fundamental physics of the QAH insulators, such as how the chiral edge transport evolves during the change of the Chern number $C$.

In quantum Hall effect, the plateau-to-plateau transition, which also corresponds to the change of the chiral edge channels (i.e., the change of $C$), is usually accessed by either sweeping the magnetic field $\mu_0 H$ or tuning the carrier density $n_{2D}$ [30–33]. Since the magnetic field $\mu_0 H$ is a

© 2022 American Physical Society

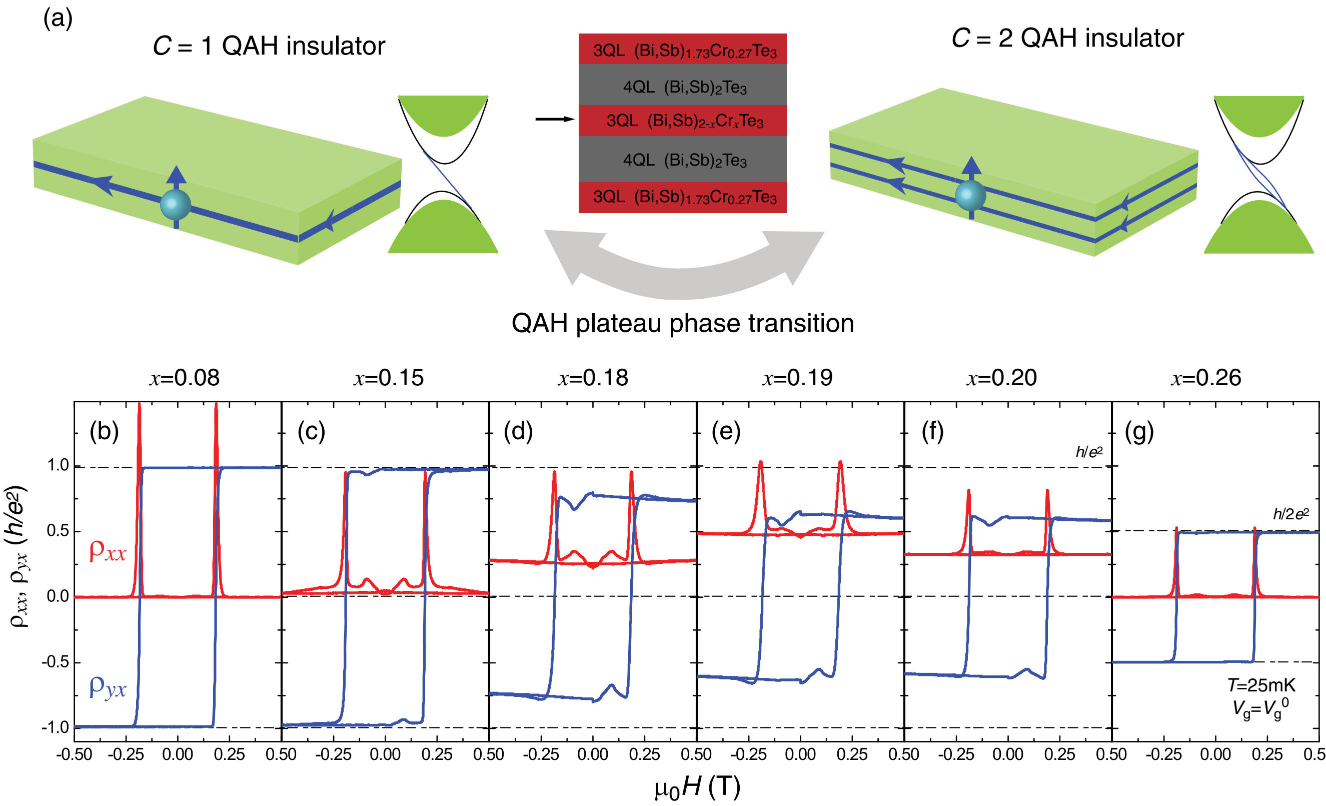

FIG. 1. QAH plateau phase transition under zero magnetic field. (a) Left (right): schematic of the $C = 1$ ($C = 2$) QAH insulator. Middle: schematic of the 3QL $(Bi, Sb)_{1.73}Cr_{0.27}Te_3$/4QL $(Bi, Sb)_2Te_3$/3QL $(Bi, Sb)_{2-x}Cr_xTe_3$/4QL $(Bi, Sb)_2Te_3$/3QL $(Bi, Sb)_{1.73}Cr_{0.27}Te_3$ pentalayer heterostructure. (b)–(g) $\mu_0 H$ dependence of $\rho_{xx}$ (red) and $\rho_{yx}$ (blue) measured at $V_g = V_g^0$ and $T = 25$ mK. $V_g^0$ values are $+4$ V, $+20$ V, $-1$ V, $-23$ V, $+14$ V, and $+20$ V for the $x = 0.08$, $x = 0.15$, $x = 0.18$, $x = 0.19$, $x = 0.20$, and $x = 0.26$, respectively.

prerequisite for the formation of the Landau levels, the $C$ change-induced plateau phase transition in quantum Hall effect occurs only under high magnetic fields [30,31]. However, in the QAH effect, the chiral edge transport appears at zero magnetic field [5,11,16,17], the systematic change of the dopant concentration, which leads to the continuous tuning of $C$ in QAH insulators, will create a plateau-to-plateau phase transition under zero magnetic field. There are two key questions regarding the plateau phase transition between $C = 1$ and $C = 2$ QAH insulators: (i) What happens to the original chiral edge channel from the initial $C = 1$ QAH insulator? (ii) How does the second chiral edge channel evolve to form the $C = 2$ QAH insulator?

In this work, we used molecular beam epitaxy (MBE) to fabricate a series of magnetic TI/TI pentalayers, specifically three quintuple layers (QL) $(Bi, Sb)_{1.73}Cr_{0.27}Te_3$/4QL $(Bi, Sb)_2Te_3$/3QL $(Bi, Sb)_{2-x}Cr_xTe_3$/4QL $(Bi, Sb)_2Te_3$/3QL $(Bi, Sb)_{1.73}Cr_{0.27}Te_3$), by systematically varying the Cr doping concentration $x$ in the middle $(Bi, Sb)_{2-x}Cr_xTe_3$ layer. Our prior study has demonstrated that the interlayer coupling between two adjacent $C = 1$ QAH insulators is weak when the thickness of the middle $(Bi, Sb)_{2-x}Cr_xTe_3$ layer with $x \geq 0.24$ is greater than 2QL [10]. We performed transport measurements and observed a plateau-to-plateau phase transition between $C = 1$ to $C = 2$ QAH insulators under zero magnetic field [Fig. 1(a)]. We found that the ratio between the Hall resistance and the longitudinal resistance under zero magnetic field is greater than 1, suggesting the sample still resides in a nonperfect QAH state at the critical point of the potential plateau phase transition [10]. This observation implies that the original chiral edge channel from the $C = 1$ QAH insulator coexists with the bulk conducting channel during the $C$ change-induced quantum phase transition.

All magnetic TI/TI pentalayer heterostructures used in this work were grown on 0.5 mm thick $SrTiO_3(111)$ substrates in an MBE chamber (Omicron Lab 10) with a base pressure $\sim 2 \times 10^{-10}$ mbar. To make all samples consistent over the entire quantum phase transition regime, we maintained the Cr doping concentration in the top and bottom magnetic TI layers at $x = 0.27$ and systematically changed $x$ in the middle 3QL $(Bi, Sb)_{2-x}Cr_xTe_3$ layer from $x = 0.08$ to $x = 0.26$ [Fig. 1(a)]. The Bi/Sb ratio in each layer was optimized to tune the chemical potential of the sample near the charge neutral point. The electrical transport measurements were carried out in a physical property measurements system (Quantum Design DynaCool, 2 K, 9 T) and a dilution refrigerator (Leiden Cryogenics, 10 mK, 9 T) with the magnetic field applied perpendicular to the film plane. Six terminal mechanically defined Hall bars

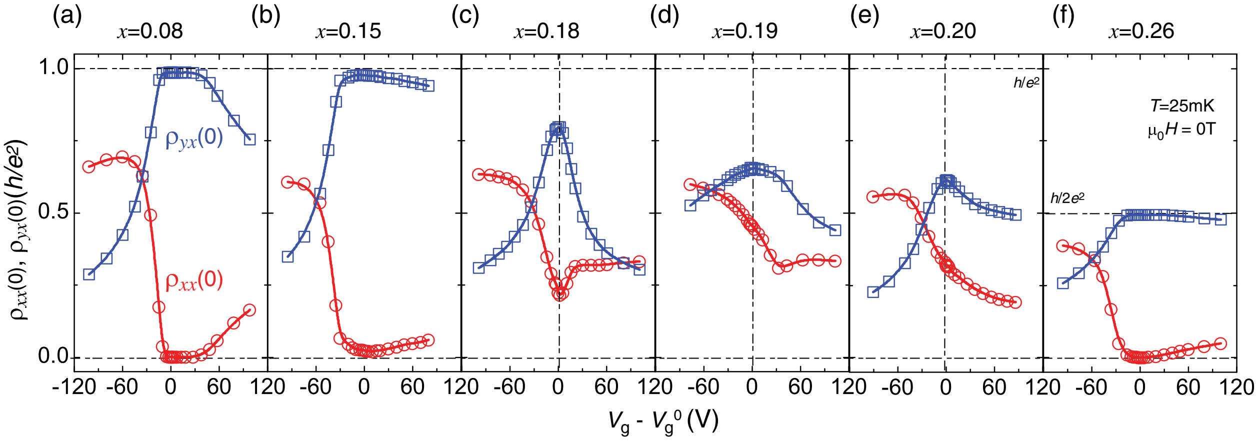

FIG. 2. Demonstration of the quantum phase transition between $C = 1$ and $C = 2$ QAH insulators. (a)–(f) $(V_g - V_g^0)$ dependence of $\rho_{yx}(0)$ (blue squares) and $\rho_{xx}(0)$ (red circles) of the magnetic TI/TI pentalayer heterostructures with $x = 0.08$ (a), $x = 0.15$ (b), $x = 0.18$ (c), $x = 0.19$ (d), $x = 0.20$ (e), and $x = 0.26$ (f). All measurements were taken at $T = 25$ mK and $\mu_0 H = 0$ T after magnetic training.

were used for electrical transport measurements. More details about the MBE growth of the samples and electrical transport measurements can be found in Supplemental Material [34].

We first performed transport measurements on these magnetic TI/TI pentalayers with different $x$ at $T = 25$ mK and $V_g = V_g^0$. The value of $V_g^0$ here is determined when the zero magnetic field Hall resistance [labeled as $\rho_{yx}$ (0)] is maximized. The $C = 1$ QAH effect is realized in a sample with $x = 0.08$ where $\rho_{yx}$ is found to be $\sim 0.986h/e^2$, and $\rho_{xx}$ is $\sim 0.0009h/e^2$ ($\sim 23\ \Omega$) under zero magnetic field [Fig. 1(b)]. For the $x = 0.15$ sample, $\rho_{yx} \sim 0.977h/e^2$ and $\rho_{xx} \sim 0.0236h/e^2$ ($\sim 600\ \Omega$) under zero magnetic field [Fig. 1(c)], slightly deviating from the perfect $C = 1$ QAH state. By steadily increasing $x$, $\rho_{yx}$ further deviates from the quantized value of $\sim h/e^2$ and finally saturates at the half-quantized value of $\sim h/2e^2$, corresponding to the potential quantum phase transition between $C = 1$ to $C = 2$ QAH insulators. $\rho_{yx}$ values are found to be $\sim 0.797h/e^2$, $\sim 0.655h/e^2$, $\sim 0.615h/e^2$, and $\sim 0.494h/e^2$ (i.e., the $C = 2$ QAH effect) for the $x = 0.18$, 0.19, 0.20, and 0.26 samples, respectively, under zero magnetic field. The corresponding values of $\rho_{xx}$ are $\sim 0.223h/e^2$, $\sim 0.456h/e^2$, $\sim 0.320h/e^2$, and $\sim 0.0015h/e^2$ ($\sim 40\ \Omega$), respectively [Figs. 1(d) to 1(g)]. The large $\rho_{xx}$ in the $x = 0.18$, 0.19, and 0.20 samples implies that the bulk conduction channels are present in these three samples in the transition region. Compared to the well-quantized $\rho_{yx}$ in both the $x = 0.08$ and 0.26 samples (i.e., the $C = 1$ and $C = 2$ QAH insulators), both $\rho_{yx}$ and $\rho_{xx}$ of the other four samples show kink features after the magnetic field $\mu_0 H$ crosses the zero magnetic field, which become more pronounced when the QAH samples are away from the quantized regimes. This kink feature is likely related to temperature rise in the sample induced by magnetic field polarity reversal during the magnetic field sweep [10,27,37]. Moreover, we noted that a topological Hall-like hump feature also appears during the magnetization reversal process in the samples that are located in the quantum phase transition regime. This observation suggests that the chiral magnetic domain walls and/or other chiral spin textures might be present in these magnetic TI heterostructures [28,38].

To further understand the plateau phase transition between $C = 1$ and $C = 2$ QAH insulators, we measured $\mu_0 H$ dependence of $\rho_{yx}$ and $\rho_{xx}$ at different $V_g$ values and plotted the $(V_g - V_g^0)$ dependence of $\rho_{yx}(0)$ and zero magnetic field $\rho_{xx}$ [labeled as $\rho_{xx}(0)$] in Fig. 2. For the $x = 0.08$ and $x = 0.26$ samples, $\rho_{yx}(0)$ exhibits a distinct plateau centered at $V_g = V_g^0$ with the quantized values of $\sim h/e^2$ and $\sim h/2e^2$, respectively. The corresponding $\rho_{xx}(0)$ shows a wide zero resistance plateau, validating the perfect $C = 1$ and $C = 2$ QAH insulator states [Figs. 2(a) and 2(f)]. For the $x = 0.15$, 0.18, 0.19, and 0.20 samples, $\rho_{yx}(0)$ shows a maximum at $V_g = V_g^0$ [Figs. 2(b) to 2(e)]. The corresponding $\rho_{xx}(0)$ shows a dip feature at $V_g = V_g^0$ for the $x = 0.15$ and 0.18 samples. For the $x = 0.19$ sample, $\rho_{xx}(0)$ also shows a dip feature centering slightly away from $V_g = V_g^0$. However, this dip feature in $\rho_{xx}(0)$ is not seen in the $x = 0.20$ sample. For the three samples located in the quantum phase transition regime, the $\rho_{yx}(0)/\rho_{xx}(0)$ ratios are 3.57, 1.44, and 1.92, corresponding to the Hall angles of 74.37°, 55.15°, and 62.51° for the $x = 0.18$, $x = 0.19$, and $x = 0.20$ samples, respectively. According to the criterion for the emergence of the QAH state, which is defined as $\rho_{yx}(0)/\rho_{xx}(0) \geq 1$, the original chiral edge channel from the $C = 1$ QAH insulator persists and never disappears in the potential phase transition region. We noted that although both the $x = 0.19$ and $x = 0.20$ samples have chiral edge transport in the nonperfect QAH regime, the misalignment between the $\rho_{yx}$ maximum and the $\rho_{xx}$ dip in the $x = 0.19$ sample and the absence of the $\rho_{xx}$ dip in the $x = 0.20$ sample are unusual. We speculated that these two behaviors might

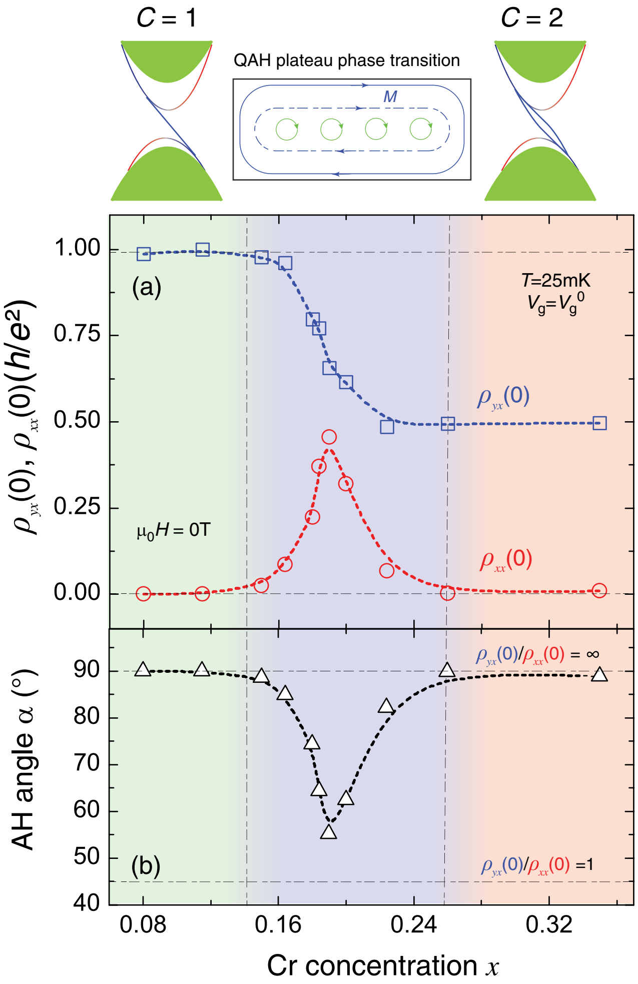

FIG. 3. Evolving chiral edge transport during the phase transition between $C = 1$ to $C = 2$ QAH insulators. (a) The Cr doping concentration $x$ dependence of $\rho_{yx}(0)$ (blue squares) and $\rho_{xx}(0)$ (red circles) of magnetic TI/TI pentalayer heterostructures measured at $V_g = V_g^0$ and $T = 25$ mK. Top: Schematic of the quantum phase transition between $C = 1$ and $C = 2$ QAH insulators. (b) $x$ dependence of the corresponding AH angle $\alpha$ [i.e., $\alpha = \arctan(\rho_{yx}(0)/\rho_{xx}(0)$, black triangles] of magnetic TI/TI pentalayer heterostructures.

be attributed to the coexistence of the chiral edge transport and the bulk conducting transport during the plateau phase transition. More studies are required to clarify their underlying physics.

Figure 3(a) shows the dependence of $\rho_{yx}(0)$ and $\rho_{xx}(0)$ on the Cr doping concentration $x$ in the middle magnetic TI layer. Eleven samples were measured at $T = 25$ mK and $V_g = V_g^0$. These eleven samples of different Cr concentrations $x$ show a systematic and smooth evolution from the $C = 1$ QAH state through the transition region and end in the $C = 2$ QAH state. If we define $\rho_{xx}(0) < 0.02h/e^2$ as the criterion for the quantized states, then the $C = 1$ and $C = 2$ QAH states are found for the $x < 0.14$ and $x > 0.26$ samples, respectively. For $0.14 \leq x \leq 0.26$, $\rho_{yx}(0)$ changes smoothly from the quantized $h/e^2$ plateau to the adjacent quantized $h/2e^2$ plateau. Concurrently, $\rho_{xx}(0)$ exhibits a peak at $x \sim 0.19$. These observations validate the $x$ change-induced quantum phase transition between $C = 1$ and $C = 2$ QAH insulators.

During the plateau phase transition regime, $\rho_{yx}(0)$ is always greater than $\rho_{xx}(0)$, i.e., $\rho_{yx}(0)/\rho_{xx}(0) > 1$ [Fig. 3(b)]. This indicates that throughout the transition, the original chiral edge channel persists and coexists with the bulk conducting channels introduced by the topological nontrivial-to-trivial phase transition in the middle magnetic TI layer [10,39,40]. In the following, we presented a phenomenological picture to understand this $x$ change-induced quantum phase transition. In magnetic TI/TI pentalayers, the total $\sigma_{xy}$ comes from the gapped Dirac bands located at the interfaces between the magnetic TI layers and the undoped TI layers. Each nontrivial interface state contributes $e^2/2h$. For the $x < 0.14$ samples, the middle magnetic TI is still located in the topological nontrivial regime and shares the same topology with the undoped TI layer, so there are two nontrivial interfaces states located at the two outer magnetic TI/TI interfaces in the pentalayers, and thus the total $\sigma_{xy} \sim e^2/h$, corresponding to the $C = 1$ QAH state. For the $x > 0.26$ samples, the middle magnetic TI becomes a trivial insulator and thus two more nontrivial interface states appear at the two inner interfaces between the undoped TI layers and the middle magnetic TI layers. The total $\sigma_{xy} \sim 2e^2/h$, corresponding to the $C = 2$ QAH state. For $0.14 \leq x \leq 0.26$, increasing $x$ makes the middle magnetic TI layer undergo a phase transition from being topological nontrivial to trivial due to the reduction of the spin-orbit coupling [10,39,40]. This topological phase transition is responsible for the occurrence of the $C$ change-induced quantum phase transition observed in magnetic TI/TI pentalayers.

To support this phenomenological picture, we performed numerical simulations on the band dispersions and wave function distributions for magnetic TI/TI pentalayers (Figs. S15 and S16) [34]. Our calculations indeed show a topological phase transition between $C = 1$ to $C = 2$ QAH states by varying the parameters that account for the exchange coupling and spin-orbit coupling strength in the middle magnetic TI layer (Fig. S15) [34]. The wave function distributions of the lowest-energy conduction bands along the $z$ direction also reveal a variation from the bulk state formed with a single peak to the interface states formed with double peaks across the phase transition (Fig. S16) [34]. This validates our phenomenological picture for the origin of the zero magnetic field plateau phase transition in magnetic TI/TI pentalayers. In addition, our theoretical calculations show the coexistence of the chiral edge channel and bulk conduction channels during the plateau phase transition between $C = 1$ and $C = 2$ QAH insulators (Fig. S17). We noted that our theoretical calculations are based on the weak interlayer interaction scenario for the formation of the $C = 2$ QAH effect. However, when the Cr

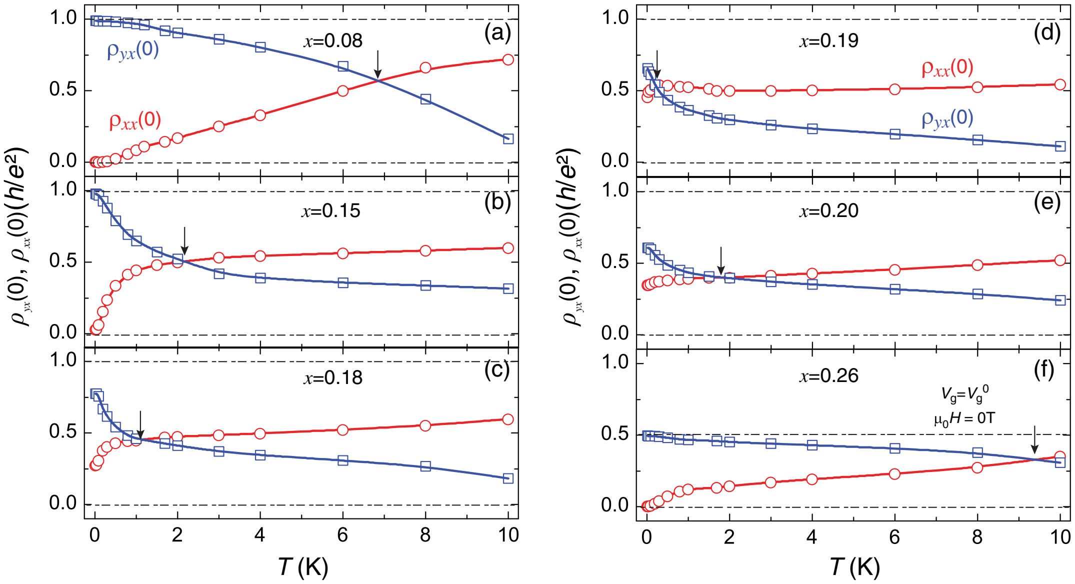

FIG. 4. Evolution of the critical temperatures of QAH insulators. (a)–(f) Temperature dependence of $\rho_{yx}(0)$ (blue squares) and $\rho_{xx}(0)$ (red circles) of magnetic TI/TI pentalayers with $x = 0.08$ (a), $x = 0.15$ (b), $x = 0.18$ (c), $x = 0.19$ (d), $x = 0.20$ (e), and $x = 0.26$ (f). All data were acquired at $\mu_0 H = 0$ T after magnetic training. The critical temperature $T_c$ (indicated by arrows) values are ~6.8 K, ~2.2 K, ~1.2 K, ~0.2 K, ~1.8 K, and ~9.2 K for the $x = 0.08$, $x = 0.15$, $x = 0.18$, $x = 0.19$, $x = 0.20$, and $x = 0.26$ samples, respectively.

doping concentration $x$ in the middle magnetic TI layers is reduced, the coupling between two adjacent $C = 1$ QAH layers is enhanced, the Weyl semimetal scenario may also apply to the formation of $C = 2$ QAH effect in our magnetic TI/TI pentalayers, particularly near the critical point of the topological phase transition [41].

Finally, we discussed the change of the critical temperatures of the QAH states within the Chern number change-induced phase transition regime. As noted above, the critical temperature $T_c$ of the QAH state is defined as the temperature at which $\rho_{yx}(0)/\rho_{xx}(0) = 1$, i.e., the crossing point of the temperature dependence of $\rho_{yx}(0)$ and $\rho_{xx}(0)$ curves (Fig. 4). The $T_c$ values of the QAH states for the six samples are shown in Figs. 1 and 2 are ~6.8 K, ~2.2 K, ~1.2 K, ~0.2 K, ~1.8 K, and ~9.2 K for the $x = 0.08$, 0.15, 0.18, 0.19, 0.20, and 0.26 samples, respectively. The decrease of $\rho_{xx}(0)$ with decreasing temperature in the $x = 0.18$, 0.19, and 0.20 samples further confirms that these three samples are still located in the nonperfect QAH regime [11,28]. During the tuning of the transition from $C = 1$ to $C = 2$ QAH states, the introduction of the bulk conducting channels in the middle TI layers obscures the original chiral edge transport from the $C = 1$ QAH state. Concomitantly, when the middle magnetic TI layer becomes a trivial insulator, the second chiral edge channel gradually emerges. This transformation completes with the sample becoming the $C = 2$ QAH insulator with two chiral edge channels. The relatively low critical temperature in the $x = 0.19$ sample at the transition critical point also supports that the original chiral edge channel is indeed affected by the appearance of the bulk conducting channels.

To summarize, we fabricated magnetic TI/TI pentalayers with different Cr doping concentrations in the middle magnetic TI layer and realized the zero magnetic field quantum phase transition between $C = 1$ to $C = 2$ QAH insulators. We found that the Hall resistance exhibits a plateau-to-plateau transition and the longitudinal resistance shows a maximum at the transition critical point. We also demonstrated that through the potential phase transition, the original chiral edge channel from the $C = 1$ QAH insulator persists and never disappears, concomitantly, the coexisting bulk conduction channels self-organize into the second chiral edge channel upon the completion of the transition. Our observation of the coexistence of the chiral edge states and the dissipative bulk conducting channels paves the way for future quantitative studies on the scaling behaviors of these novel quantum phase transitions in QAH insulators and also lays down the necessary conditions and limitations on how the QAH insulators can be utilized in next-generation electronic and spintronic devices with low power consumption.

We thank Yongtao Cui, Nitin Samarth, Di Xiao, Xiaodong Xu, and Jiaqiang Yan for helpful discussions. The work is primarily supported by DOE Grant No. DE-SC0019064, including the MBE growth, the dilution temperature electrical transport measurements, and the theoretical support. The PPMS measurements were partially supported by ARO Young Investigator Program Grant No. W911NF1810198, NSF-CAREER Grant No. DMR-1847811, and the Gordon and Betty Moore Foundation's EPiQS Initiative (No. GBMF9063 to C.-Z. C.). Part of the measurements at dilution-refrigerator temperature is supported by NSF Grant No. DMR-1707340.

[*]Corresponding author.
cxc955@psu.edu
[†]Y.-F. Z. and R. Z. contributed equally.

[1] M. Z. Hasan and C. L. Kane, Colloquium: Topological insulators, Rev. Mod. Phys. **82**, 3045 (2010).

[2] X. L. Qi and S. C. Zhang, Topological insulators and superconductors, Rev. Mod. Phys. **83**, 1057 (2011).

[3] F. D. M. Haldane, Model for a Quantum Hall-Effect without Landau Levels: Condensed-Matter Realization of the "Parity Anomaly", Phys. Rev. Lett. **61**, 2015 (1988).

[4] R. Yu, W. Zhang, H. J. Zhang, S. C. Zhang, X. Dai, and Z. Fang, Quantized anomalous Hall effect in magnetic topological insulators, Science **329**, 61 (2010).

[5] C. Z. Chang *et al.*, Experimental observation of the quantum anomalous Hall effect in a magnetic topological insulator, Science **340**, 167 (2013).

[6] C. X. Liu, X. L. Qi, X. Dai, Z. Fang, and S. C. Zhang, Quantum Anomalous Hall Effect in $\mathrm{Hg_{1-y}Mn_yTe}$ Quantum Wells, Phys. Rev. Lett. **101**, 146802 (2008).

[7] X. L. Qi, T. L. Hughes, and S. C. Zhang, Topological field theory of time-reversal invariant insulators, Phys. Rev. B **78**, 195424 (2008).

[8] D. J. Thouless, M. Kohmoto, M. P. Nightingale, and M. Dennijs, Quantized Hall Conductance in a Two-Dimensional Periodic Potential, Phys. Rev. Lett. **49**, 405 (1982).

[9] H. M. Weng, R. Yu, X. Hu, X. Dai, and Z. Fang, Quantum anomalous Hall effect and related topological electronic states, Adv. Phys. **64**, 227 (2015).

[10] Y. F. Zhao, R. Zhang, R. Mei, L. J. Zhou, H. Yi, Y. Q. Zhang, J. Yu, R. Xiao, K. Wang, N. Samarth, M. H. W. Chan, C. X. Liu, and C. Z. Chang, Tuning the Chern number in quantum anomalous Hall insulators, Nature (London) **588**, 419 (2020).

[11] C. Z. Chang, W. W. Zhao, D. Y. Kim, H. J. Zhang, B. A. Assaf, D. Heiman, S. C. Zhang, C. X. Liu, M. H. W. Chan, and J. S. Moodera, High-precision realization of robust quantum anomalous Hall state in a hard ferromagnetic topological insulator, Nat. Mater. **14**, 473 (2015).

[12] C. Z. Chang, W. W. Zhao, D. Y. Kim, P. Wei, J. K. Jain, C. X. Liu, M. H. W. Chan, and J. S. Moodera, Zero-Field Dissipationless Chiral Edge Transport and the Nature of Dissipation in the Quantum Anomalous Hall State, Phys. Rev. Lett. **115**, 057206 (2015).

[13] H. Polshyn, J. Zhu, M. A. Kumar, Y. Zhang, F. Yang, C. L. Tschirhart, M. Serlin, K. Watanabe, T. Taniguchi, A. H. MacDonald, and A. F. Young, Electrical switching of magnetic order in an orbital Chern insulator, Nature (London) **588**, 66 (2020).

[14] Y. Deng, Y. Yu, M. Z. Shi, Z. Guo, Z. Xu, J. Wang, X. H. Chen, and Y. Zhang, Quantum anomalous Hall effect in intrinsic magnetic topological insulator $\mathrm{MnBi_2Te_4}$, Science **367**, 895 (2020).

[15] C. Z. Chang and M. D. Li, Quantum anomalous Hall effect in time-reversal-symmetry breaking topological insulators, J. Phys.: Condens. Matter **28**, 123002 (2016).

[16] J. G. Checkelsky, R. Yoshimi, A. Tsukazaki, K. S. Takahashi, Y. Kozuka, J. Falson, M. Kawasaki, and Y. Tokura, Trajectory of the anomalous Hall effect towards the quantized state in a ferromagnetic topological insulator, Nat. Phys. **10**, 731 (2014).

[17] X. F. Kou, S. T. Guo, Y. B. Fan, L. Pan, M. R. Lang, Y. Jiang, Q. M. Shao, T. X. Nie, K. Murata, J. S. Tang, Y. Wang, L. He, T. K. Lee, W. L. Lee, and K. L. Wang, Scale-Invariant Quantum Anomalous Hall Effect in Magnetic Topological Insulators beyond the Two-Dimensional Limit, Phys. Rev. Lett. **113**, 137201 (2014).

[18] M. Serlin, C. L. Tschirhart, H. Polshyn, Y. Zhang, J. Zhu, K. Watanabe, T. Taniguchi, L. Balents, and A. F. Young, Intrinsic quantized anomalous Hall effect in a moiré heterostructure, Science **367**, 900 (2020).

[19] C. Z. Chang, W. W. Zhao, J. Li, J. K. Jain, C. X. Liu, J. S. Moodera, and M. H. W. Chan, Observation of the Quantum Anomalous Hall Insulator to Anderson Insulator Quantum Phase Transition and Its Scaling Behavior, Phys. Rev. Lett. **117**, 126802 (2016).

[20] C. X. Liu, S. C. Zhang, and X. L. Qi, The quantum anomalous Hall effect: Theory and experiment, Annu. Rev. Condens. Matter Phys. **7**, 301 (2016).

[21] D. Xiao, J. Jiang, J. H. Shin, W. B. Wang, F. Wang, Y. F. Zhao, C. X. Liu, W. D. Wu, M. H. W. Chan, N. Samarth, and C. Z. Chang, Realization of the Axion Insulator State in Quantum Anomalous Hall Sandwich Heterostructures, Phys. Rev. Lett. **120**, 056801 (2018).

[22] M. Mogi, M. Kawamura, A. Tsukazaki, R. Yoshimi, K. S. Takahashi, M. Kawasaki, and Y. Tokura, Tailoring tricolor structure of magnetic topological insulator for robust axion insulator, Sci. Adv. **3**, eaao1669 (2017).

[23] S. Grauer, S. Schreyeck, M. Winnerlein, K. Brunner, C. Gould, and L. W. Molenkamp, Coincidence of superparamagnetism and perfect quantization in the quantum anomalous Hall state, Phys. Rev. B **92**, 201304(R) (2015).

[24] S. Grauer, K. M. Fijalkowski, S. Schreyeck, M. Winnerlein, K. Brunner, R. Thomale, C. Gould, and L. W. Molenkamp, Scaling of the Quantum Anomalous Hall Effect as an Indicator of Axion Electrodynamics, Phys. Rev. Lett. **118**, 246801 (2017).

[25] A. Kandala, A. Richardella, S. Kempinger, C. X. Liu, and N. Samarth, Giant anisotropic magnetoresistance in a quantum anomalous Hall insulator, Nat. Commun. **6**, 7434 (2015).

[26] Y. Ou, C. Liu, G. Jiang, Y. Feng, D. Zhao, W. Wu, X. X. Wang, W. Li, C. Song, L. L. Wang, W. Wang, W. Wu, Y. Wang, K. He, X. C. Ma, and Q. K. Xue, Enhancing the quantum anomalous Hall effect by magnetic codoping in a topological insulator, Adv. Mater. **30**, 1703062 (2018).

[27] A. J. Bestwick, E. J. Fox, X. F. Kou, L. Pan, K. L. Wang, and D. Goldhaber-Gordon, Precise Quantization of the Anomalous Hall Effect near Zero Magnetic Field, Phys. Rev. Lett. **114**, 187201 (2015).

[28] J. Jiang, D. Xiao, F. Wang, J. H. Shin, D. Andreoli, J. X. Zhang, R. Xiao, Y. F. Zhao, M. Kayyalha, L. Zhang, K. Wang, J. D. Zang, C. X. Liu, N. Samarth, M. H. W. Chan, and C. Z. Chang, Concurrence of quantum anomalous Hall and topological Hall effects in magnetic topological insulator sandwich heterostructures, Nat. Mater. **19**, 732 (2020).

[29] W. B. Wang, Y. B. Ou, C. Liu, Y. Y. Wang, K. He, Q. K. Xue, and W. D. Wu, Direct evidence of ferromagnetism in a quantum anomalous hall system, Nat. Phys. **14**, 791 (2018).

[30] A. M. M. Pruisken, Universal Singularities in the Integral Quantum Hall-Effect, Phys. Rev. Lett. **61**, 1297 (1988).

[31] H. P. Wei, D. C. Tsui, M. A. Paalanen, and A. M. M. Pruisken, Experiments on Delocalization and Universality in the Integral Quantum Hall-Effect, Phys. Rev. Lett. **61**, 1294 (1988).

[32] W. L. Li, G. A. Csathy, D. C. Tsui, L. N. Pfeiffer, and K. W. West, Scaling and Universality of Integer Quantum Hall Plateau-to-Plateau Transitions, Phys. Rev. Lett. **94**, 206807 (2005).

[33] W. L. Li, C. L. Vicente, J. S. Xia, W. Pan, D. C. Tsui, L. N. Pfeiffer, and K. W. West, Scaling in Plateau-to-Plateau Transition: A Direct Connection of Quantum Hall Systems with the Anderson Localization Model, Phys. Rev. Lett. **102**, 216801 (2009).

[34] See Supplemental Material at http://link.aps.org/supplemental/10.1103/PhysRevLett.128.216801 for further details regarding the MBE growth, sample characterizations, more transport results, and theoretical calculations, which includes Refs. [35,36].

[35] A. Arrott, Criterion for ferromagnetism from observations of magnetic isotherms, Phys. Rev. **108**, 1394 (1957).

[36] C.-X. Liu, X.-L. Qi, H. Zhang, X. Dai, Z. Fang, and S.-C. Zhang, Model Hamiltonian for topological insulators, Phys. Rev. B **82**, 045122 (2010).

[37] K. Yasuda, A. Tsukazaki, R. Yoshimi, K. Kondou, K. S. Takahashi, Y. Otani, M. Kawasaki, and Y. Tokura, Current-Nonlinear Hall Effect and Spin-Orbit Torque Magnetization Switching in a Magnetic Topological Insulator, Phys. Rev. Lett. **119**, 137204 (2017).

[38] R. Xiao, D. Xiao, J. Jiang, J. H. Shin, F. Wang, Y. F. Zhao, R. X. Zhang, A. Richardella, K. Wang, M. Kayyalha, M. H. W. Chan, C. X. Liu, C. Z. Chang, and N. Samarth, Mapping the phase diagram of the quantum anomalous Hall and topological Hall effects in a dual-gated magnetic topological insulator heterostructure, Phys. Rev. Research **3**, L032004 (2021).

[39] J. S. Zhang, C. Z. Chang, P. Z. Tang, Z. C. Zhang, X. Feng, K. Li, L. L. Wang, X. Chen, C. X. Liu, W. H. Duan, K. He, Q. K. Xue, X. C. Ma, and Y. Y. Wang, Topology-driven magnetic quantum phase transition in topological insulators, Science **339**, 1582 (2013).

[40] C. Z. Chang, P. Z. Tang, Y. L. Wang, X. Feng, K. Li, Z. C. Zhang, Y. Y. Wang, L. L. Wang, X. Chen, C. X. Liu, W. H. Duan, K. He, X. C. Ma, and Q. K. Xue, Chemical-Potential-Dependent Gap Opening at the Dirac Surface States of $Bi_2Se_3$ Induced by Aggregated Substitutional Cr Atoms, Phys. Rev. Lett. **112**, 056801 (2014).

[41] A. A. Burkov and L. Balents, Weyl Semimetal in a Topological Insulator Multilayer, Phys. Rev. Lett. **107**, 127205 (2011).